The Precise Measurement of Free-Form Surfaces

by

William Wolovich[1], Hassan Albakri and Hulya Yalcin

Abstract

We outline a new procedure for measuring free-form curves and surfaces using implicit polynomial equations. Such equations have long been known to offer certain advantages over the more traditional parametric methods. However, the lack of general procedures for obtaining implicit polynomial models of higher degree, which precisely represent arbitrary 3-D shapes, have prevented their general use in many practical applications, including rapid and precise metrology. Recent mathematical advances obtained at Brown University, experimentally verified using a state-of-the-art Chameleon coordinate measuring machine, have demonstrated potential advantages of implicit methods for modeling and measuring a variety of manufactured objects.

1 Introduction

Free-form surfaces, which are also called sculptured, contoured or organic, are ubiquitous in our daily lives. Examples include airfoils, automobile bodies, ship propellers, turbine blades, geographical contours and animal organs. Such surfaces may be observed visually or sensed tactily. They may exist only in the mind of a designer or in the memory of a computer. In many different applications, such as reverse engineering, industrial design, inspection and metrology, computer vision, and computer aided geometric design, free-form surfaces must be modeled, identified, aligned, compared (to other objects), modified, fabricated and measured.

Unlike objects that are composed of simple geometric *primitives*, such as planes, lines, spheres and cylinders, free-form objects often have no obvious *feature points*. Therefore, they are more difficult to define and model mathematically than simple geometric objects. In most cases today, *parametric equations* are used to model small patches of free-form surfaces, which are then pieced together to insure certain smoothness conditions at the patch boundaries. This modeling requires some rather involved and sophisticated mathematical techniques, such

[1]Professor of Engineering, Brown University, Box D, Providence, RI 02912. This work was supported by the NSF under Grant DMI-9820804 and by Brown & Sharpe Measuring Systems.

as Bézier curves and surfaces, Coons patches, B-splines and NURBS (non-uniform rational B-splines)[1, 2, 3].

Many researchers have studied the fitting of measured points to nominal geometries using such procedures. Patrikalakis and Bardis [4] developed data localization for NURBS surfaces, and proposed an algorithm to construct a tolerance zone on a NURB surface patch. Their part conformation is done by a least squares fit and compared to the tolerance zone. Later, Tuohy et al.[5] developed a representation based on interval B-splines to deal with uncertainty on non-linear geometric models.

Wang proposed a minimum zone evaluation algorithm based on a minimax fit[6], subsequently proposing a method to estimate the critical parameters of manufactured part models from CMM data based on the evaluation of form tolerances by model fitting. This procedure employs a minimization of the sum of squared distances of the measured points from the surface of the model with respect to the model parameters[7]. The shape of the constructed model is allowed to vary within a prescribed domain in which the shape parameters are defined. Choi and Kurfess present another zone evaluation algorithm which places the sampled data points within a specified tolerance range[8]. They then extend the zone fitting to a minimum zone evaluation[9].

Least squares and extreme fits are often used in numerical coordinate data analysis, and various researchers have developed a number of numerical algorithms for three dimensional data analysis. Sahoo and Menq formalized the uncertainty in measured data analysis and proposed a data localization algorithm based on a least squares fit. They also addressed the robustness of their algorithm[10]. Kurfess and Banks formulated the underlying concept in a more statistical approach by developing a statistical relationship to determine the validity of geometric models[11]. In [12], Kurfess and Choi suggest a methodology to evaluate the uncertainty in an extreme fit based on a method which estimates the extreme fit evaluation error by re-sampling and a bootstrap replication of the extreme fit evaluations.

Generally speaking, there are problems associated with virtually any measurement algorithms, and no single procedure can handle all of the problems associated with free-form surfaces. In particular, precise alignment and measurement can be difficult[13], fabrication may be questionable[14], modifications are generally local, rather than global[1], and the measurement of surface points often requires iterative approximations. In this report, we will present a new, alternative approach to free-form surface measurement which offers some benefits compared to the more traditional methods noted above, especially from the point of view of simplicity and computational speed.

2 Implicit Representations

In the past few years, *implicit representations* have been used more frequently, allowing a better treatment of several problems. One example is the point classification problem, which is easily solved with the implicit representation. It consists of a simple evaluation of the implicit functions, although the determination of the distance error between the measured and the model surface is considerably more involved. Furthermore, implicit representations imply surfaces of desired smoothness with the lowest possible degree. Finally, when we restrict ourselves to polynomial functions, the implicit representation is more general than the parametric representation. Indeed, it is well known that parametric equations can be converted to implicit ones through the process of *implicitization*[15, 16], but not always the reverse.

Our ultimate goal in this report is to measure the error between points collected on a model blade and corresponding points collected from other "identical" blades. Clearly, it is difficult to compute such errors directly from the points, since it requires determining which points on the model blade correspond to which points on the other blades. To ameliorate this difficulty, we fit implicit polynomials to the points collected on the model blade and compute the perpendicular distance from this implicit polynomial model to measured points on the other blades. Although the implicit polynomial fit to the points on the model blade does not "exactly" represent the curve that passes through these points, it is a very good approximation, and certainly one that can be used to precisely determine the position errors of the other blades relative to the model blade, as we will show.

We might note that there is very little in the literature on higher degree IP models for large or entire free-form shapes because of the lack of tractable computational procedures for obtaining and analyzing such models[17]. However, over the past two years, we have obtained some significant new results relative to free-form objects defined by *implicit polynomial* (IP) equations of (arbitrary) degree n, namely

$$F_n(x,y,z) = \sum_{0 \leq i+j+k \leq n} a_{ijk} x^i y^j z^k = 0$$

As a result of our investigations, we have developed several useful new procedures and computer programs for describing and analyzing them[18, 19, 20, 21, 22, 23, 24]. Here, we extend and embellish these earlier results to include the precise measurement of 3-D free-form surfaces.

Our measurement procedures are *model-based*, in the sense that they require initial IP models of free-form surfaces. Unfortunately, the implicit polynomial equation(s) which define an arbitrary free-form surface are not easily determined. A "brute force" but highly impractical method would be to alter the coefficients a_{ijk} of $F_n(x,y,z)$ until a desired shape is obtained. Alternatively, one could "fit" some mathematical equation to a set of data points which outline the boundary of a given shape[25, 26, 27, 28]. The ability to obtain accurate and robust mathematical expressions for given boundary data sets is a fundamental and difficult problem in reverse engineering. Although several different fitting algorithms have been proposed thus far, the computational cost of most of them is quite high because of the nonlinear optimization procedures required to obtain acceptable fits.

Much recent research at Brown University has focused on fitting IP equations to 2-D and 3-D boundary data sets[25, 27]. These efforts have produced a new fitting algorithm, which we will employ, called *3L fitting*[25], which is relatively stable and fast, since it involves an explicit, least-squares computation. 3L fitting also allows one to vary a level set on either side of a set of planar boundary points until an optimal fitting accuracy is obtained.

In particular, consider an ordered, closed set, Γ_0, of N_0 planar data points (x_i, y_i) which one would like to model as the zero set of (say) a fourth degree implicit polynomial

$$F_4(x,y) = \sum_{0 \le i+j \le 4} a_{ij} x^i y^j = m^T(x,y)a,$$

where the 15 component vector

$$m^T(x,y) = \begin{bmatrix} 1 \; x \; y \; x^2 \; xy \; y^2 \; x^3 \; x^2y \; xy^2 \; y^3 \; x^4 \; x^3y \; x^2y^2 \; xy^3 \; y^4 \end{bmatrix},$$

and the corresponding 15 component vector

$$a = \begin{bmatrix} a_{00} \; a_{10} \; a_{01} \; a_{20} \; a_{11} \; a_{02} \; a_{30} \; a_{21} \; a_{12} \; a_{03} \; a_{40} \; a_{31} \; a_{22} \; a_{13} \; a_{04} \end{bmatrix}^T$$

If each $(i-th)$ row of the matrix M_{Γ_0} is defined as $m^T(x_i, y_i)$, then as shown in [25], the minimization of $E = \sum_{(x,y)\in\Gamma_0} F_4(x,y)$ is equivalent to the minimization of $E = a^T M_{\Gamma_0}^T M_{\Gamma_0} a$.

Unfortunately, this "1L" minimization procedure often fails to produce an acceptable IP fit to a set of data points, and much better results are obtained if one introduces two fictitious data sets close to Γ_0, one set Γ_{+c} of N_{+c} points an algebraic distance c outside Γ_0 and the other set Γ_{-c} of N_{-c} points an algebraic distance c inside Γ_0.

One next defines the $(N_{-c} + N_0 + N_{-c}) \times 15$ *three level-set* (3L) matrix

$$M_{3L} \stackrel{def}{=} \begin{bmatrix} M_{\Gamma_{-c}} \\ M_{\Gamma_0} \\ M_{\Gamma_{+c}} \end{bmatrix},$$

and the corresponding $N_{-c} + N_0 + N_{+c}$ component column vector

$$b \stackrel{def}{=} \begin{bmatrix} -c \\ 0 \\ +c \end{bmatrix},$$

so that $M_{3L}a = b$. It then follows[25] that the pseudo-inverse solution for the $F_4(x,y)$ coefficient vector

$$a = (M_{3L}^T M_{3L})^{-1} M_{3L}^T b$$

generally implies a numerically stable and robust IP fit to the given data set Γ_0. A very detailed development and explanation of this 3L fitting algorithm is given in [25].

3 Objects with Repetitive Shapes

One often must compare several (ideally) identical objects to each other or to a model object, such as the turbine blades in a jet engine, the propeller blades of a ship, or the contoured grooves in a gear. If the profile and tooth trace errors of a gear exceed tolerance errors, the running qualities of the gear decrease significantly, causing increased tip wear that can seriously degrade overall gear performance[29]. More serious consequences can occur if the turbine blades in a jet engine are not precisely and identically fabricated.

A two step procedure will now be employed to quantify the differences between the three blades of a ship propeller, the first being defined as the model blade. This would not be necessary if one had the IP equations of a model blade to begin with. However, it is assumed here that one does not have such a priori information, so that one of the propeller blades must be measured then modeled to define an "ideal" IP model for all three.

Figure 1 depicts a Brown & Sharpe Chameleon coordinate measuring machine being used to determine surface points on a 3-blade propeller. Initial measurements were used to obtain 2-D sets of (y, z) data points along five parallel profiles of the *model blade* A perpendicular to the x axis. By varying the level sets on either side of the data sets, the 3L fitting algorithm[25] was used to obtain the quartic ($4th$ degree) IP equations that follow, whose zero sets closely model points on the parallel profiles.

The (red) 3L fit of the (blue) measured points for profile 1 of blade A is defined by the implicit polynomial equation: $y^4 - 0.088y^3z + 2.083y^2z^2 - 4.805yz^3 + 1.741z^4 + 14.531y^3 - 15.653y^2z - 17.377yz^2 - 2.704z^3 - 87.629y^2 + 4.574yz - 201.26z^2 - 950.35y + 138.09z + 5146.7 = 0$, and depicted in Figure 2.

The (red) fit of the (blue) measured points for profile 3 of blade A is defined by the implicit polynomial equation: $y^4 - 1.038y^3z + 3.041y^2z^2 - 3.765yz^3 + 1.922z^4 + 15.833y^3 - 31.942y^2z + 29.537yz^2 - 25.706z^3 - 102.36y^2 + 29.709yz - 187.493z^2 - 1522.1y + 1811.3z + 9445.3 = 0$,

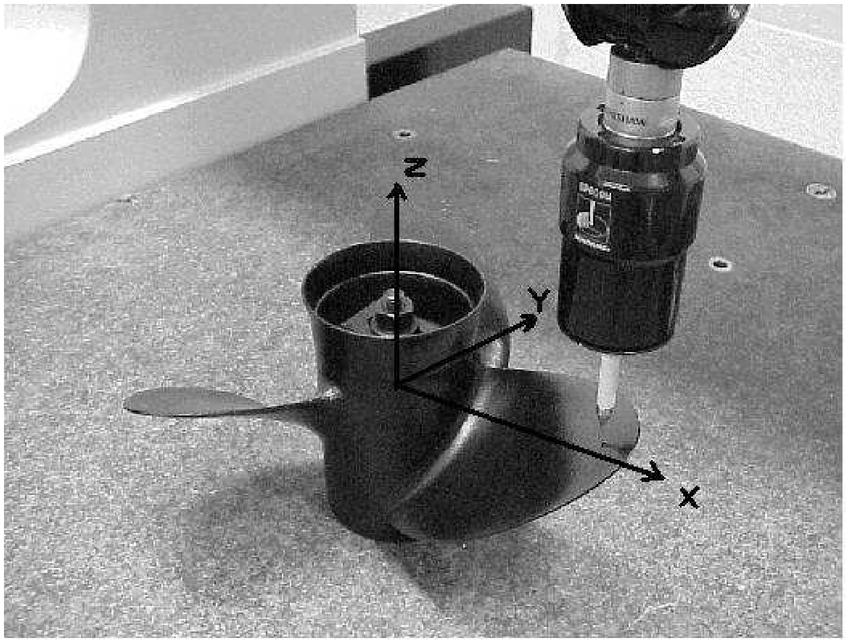

Figure 1: A Closer View (Model) Blade A Measurements

and depicted in Figure 2.

The (red) fit of the (blue) measured points for profile 5 of blade A is defined by the implicit polynomial equation: $y^4 + 1.453y^3z - 7.594y^2z^2 + 6.431yz^3 + 0.97z^4 - 17.437y^3 + 29.452y^2z + 7.7yz^2 - 26.845z^3 + 371.463y^2 - 736.448yz - 20.391z^2 - 3088.1y + 2226.6z + 7559.2 = 0$, and depicted in Figure 2.

These 3 quartic IPs represent the equations that define the model blade A. The contours of blades B and C will be compared to those of blade A by using these equations and those of the other two profiles, 2 and 4, which are not given explicitly in this report. Unless otherwise noted, the horizontal and vertical distance units depicted on all of these comparison figures are in centimeters (cm).

To determine "how close" the measured points of all 3 blades fit the IP model, one must determine the Euclidean distance from any measured point to the IP curve. As noted in

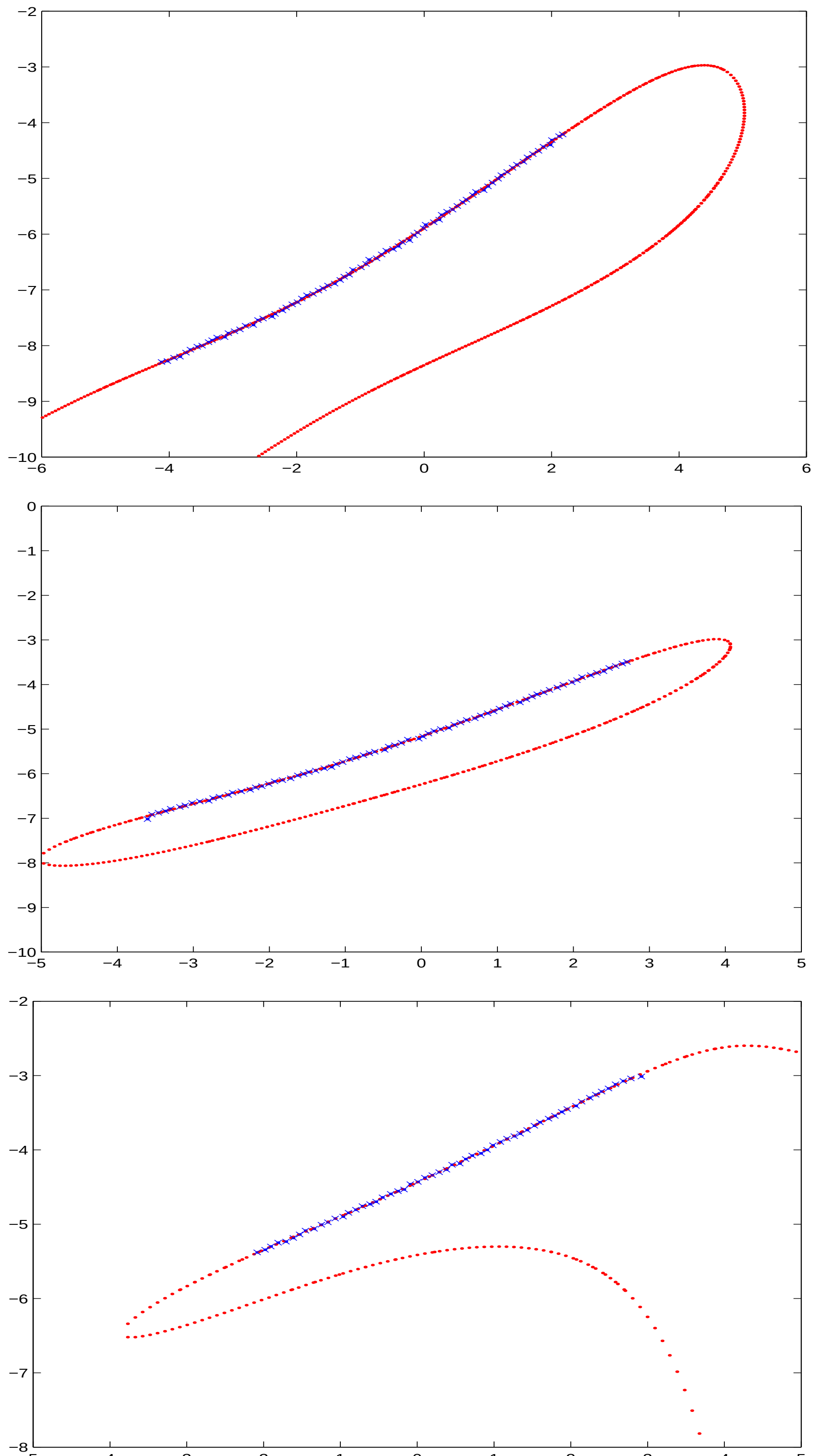

Figure 2: Red 3L IP Fits of Blue Measured Profiles 1 (Top), 3 (Middle) and 5 (Bottom)

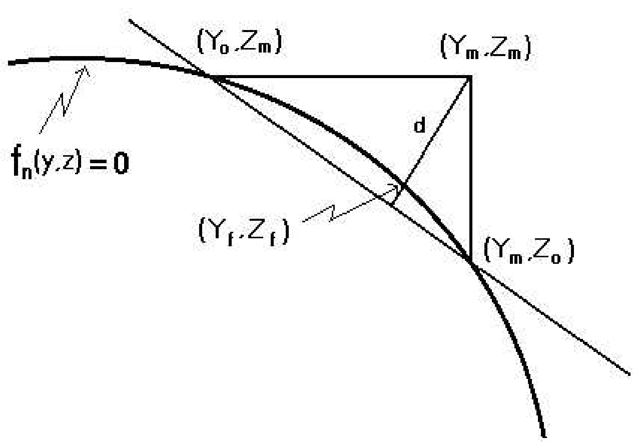

Figure 3: Determining $\approx$ 2-D $\perp$ Distance Errors

[30], this distance cannot be computed directly. Therefore, one must use either an iterative procedure[2] or an approximation. In [30], Taubin employs an approximate distance defined by a "scaled" algebraic distance, namely $|F_n(x,y)|/\parallel \bigtriangledown F_n(x,y) \parallel$. In this report, an alternative approximation will be used because (a) it is faster than iteration and (b) it produced distance approximation errors less than .001 mm in the experiments, while Taubin's procedure could yield distance errors greater than .01 mm.

To illustrate our distance approximation procedure, consider Figure 3, where (y_m, z_m) denotes any measured point, and $f_n(y,z) = 0$ represents any one of our red model IP approximations to the blue data points depicted in Figure 2. The points (y_0, z_m) and (y_m, z_0) are the perpendicular projections of the measured point onto the IP curve. To determine these points, we substitute the measured z_m for z into $f_n(y,z) = 0$, which implies a polynomial function of y alone. We then solve for y_0 using Newton's successive approximation root-finding procedure, which converges very fast.

[2]One such procedure, suggested by a reviewer, is to choose $y_1 = y_0$ and $z_1 = z_m$ as initial values in an iterative scheme defined by $y_{k+1} = y_k - F_n(y_k, z_k)/ \bigtriangledown_y F_n(y_k, z_k)$ and $z_{k+1} = z_k - F_n(y_k, z_k)/ \bigtriangledown_z F_z(y_k, z_k)$.

The line through (y_0, z_m) and (y_m, z_0) is then defined by:

$$det \begin{bmatrix} y - y_0 & z - z_m \\ y_m - y_0 & z_0 - z_m \end{bmatrix} = (z_m - z_0)(y - y_0) + (y_m - y_0)(z - z_m) = 0,$$

which implies that the line through (y_m, z_m) perpendicular to this line is defined by:

$$\frac{y - y_m}{z_m - z_0} = \frac{z - z_m}{y_m - y_0} \quad \Longrightarrow \quad z = \left(\frac{y_m - y_0}{z_m - z_0} \right) (y - y_m) + z_m$$

Substituting this value for z into $f_n(y, z) = 0$ implies a polynomial function of y alone which then is solved for y_f using Newton's successive approximation root-finding procedure, as above. The corresponding z_f point is then given by $z_f = (y_m - y_0)(y_f - y_0)/(z_m - z_0) + z_m$.

Since the point (y_f, z_f) lies on both the IP curve and the perpendicular line from the measured point to the line between (y_0, z_m) and (y_m, z_0), our approximation to the distance between (y_m, z_m) and the IP curve is given by

$$d = \sqrt{(y_m - y_f)^2 + (z_m - z_f)^2},$$

which is shown in Figure 3.

This procedure was used to determine the perpendicular distances from the measured points on profiles 1, 3 and 5 of all three propeller blades to the red IP models defined by blade A. Analogous, parallel profiles of all blades were obtained by consecutively rotating our Cartesian coordinate system 120^0 about the vertical (z axis) and repeating measurement trajectories in parallel (y, z)-planes 10 cm apart in the x direction (see Figure 1). Contour differences between blades B and C, relative to the model blade A, were quantified in this manner, as depicted in Figures 4, 5 and 6.

Clearly, the distance errors are the smallest for all three profiles of the model blade A. These errors (centered at 0) are due more to the surface irregularities associated with the actual propeller blades used in our experiments than to our distance approximation formula. Also, inherent CMM measurement errors are always introduced because CMMs typically record the probe location at the center of the stylus ball instead of the point where it actually touches the surface.

What is of primary significance, however, is how Figure 4 indicates that profile 1 of blade B is slightly below (0.4mm) that of blade A, while profile 1 of blade C is slightly above (0.4mm) that of blade A. Profiles 3 and 5 of blades B and C display a continual degradation in these directions; i.e. profile 3 of blade B is approximately 0.8mm below that of the model blade, and profile 5 of blade B is over 1mm below that the model. Profiles 3 and 5 of blade C display that its shape diverges away from the model shape with increasing distance from the vertical axis.

4 3-D Interpolated IP Surfaces

In certain situations, one might want to determine the distance errors for blades B and C, relative to the model blade A, at arbitrary points or along arbitrary (x, y, z) trajectories on the blade surface, and not only along the 5 previously defined (y, z) profiles. This objective can be achieved using interpolation. In particular, by interpolating the 2-D IP equations of a sequence of parallel, two-dimensional profiles of a 3-D surface, IP equations of the entire surface can be obtained[31, 32, 14, 33, 34].

For example, a single IP equation can be used to model the entire 3-D surface of a free-form object defined between (say) two profiles that are perpendicular to an x axis of orientation. In particular, if

$$F_a(y, z) = \sum_{0 \leq i+j \leq n} a_{ij} y^i z^j = 0$$

and

$$F_b(y, z) = \sum_{0 \leq i+j \leq n} b_{ij} y^i z^j = 0$$

define two adjacent parallel profiles, then the 3D implicit polynomial

$$F_{n+1}(x, y, z) = \sum_{0 \leq i+j \leq n} (\alpha_{ij} + x\beta_{ij}) y^i z^j = 0,$$

where $\alpha_{ij} = (a_{ij} x_b - b_{ij} x_a)/(x_b - x_a)$ and $\beta_{ij} = (b_{ij} - a_{ij})/(x_b - x_a)$, will define a *linearly interpolated* surface between the profiles, because $F_{n+1}(x_a, y, z) = F_a(y, z)$ and $F_{n+1}(x_b, y, z) =$

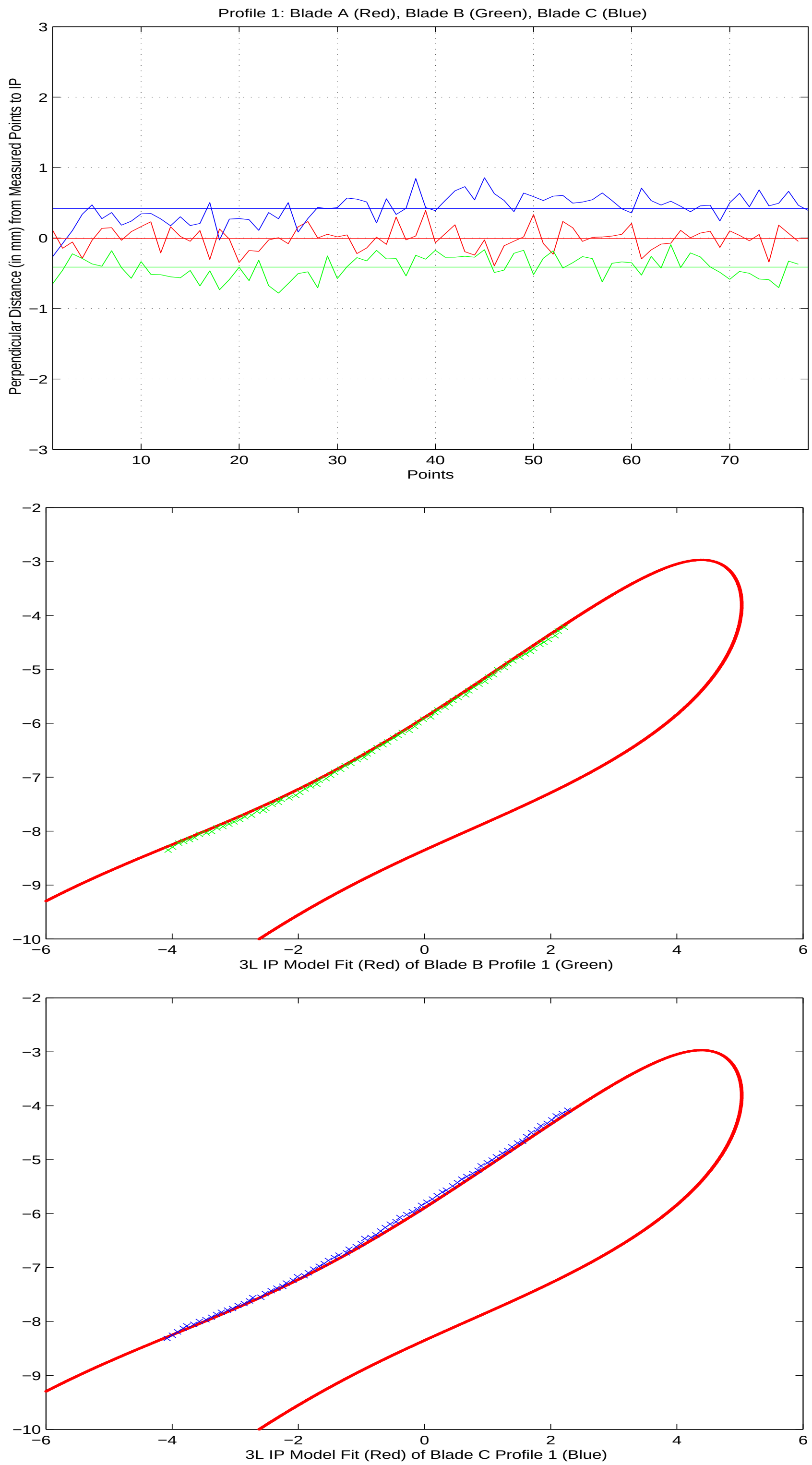

Figure 4: Profile 1 Perpendicular Distances

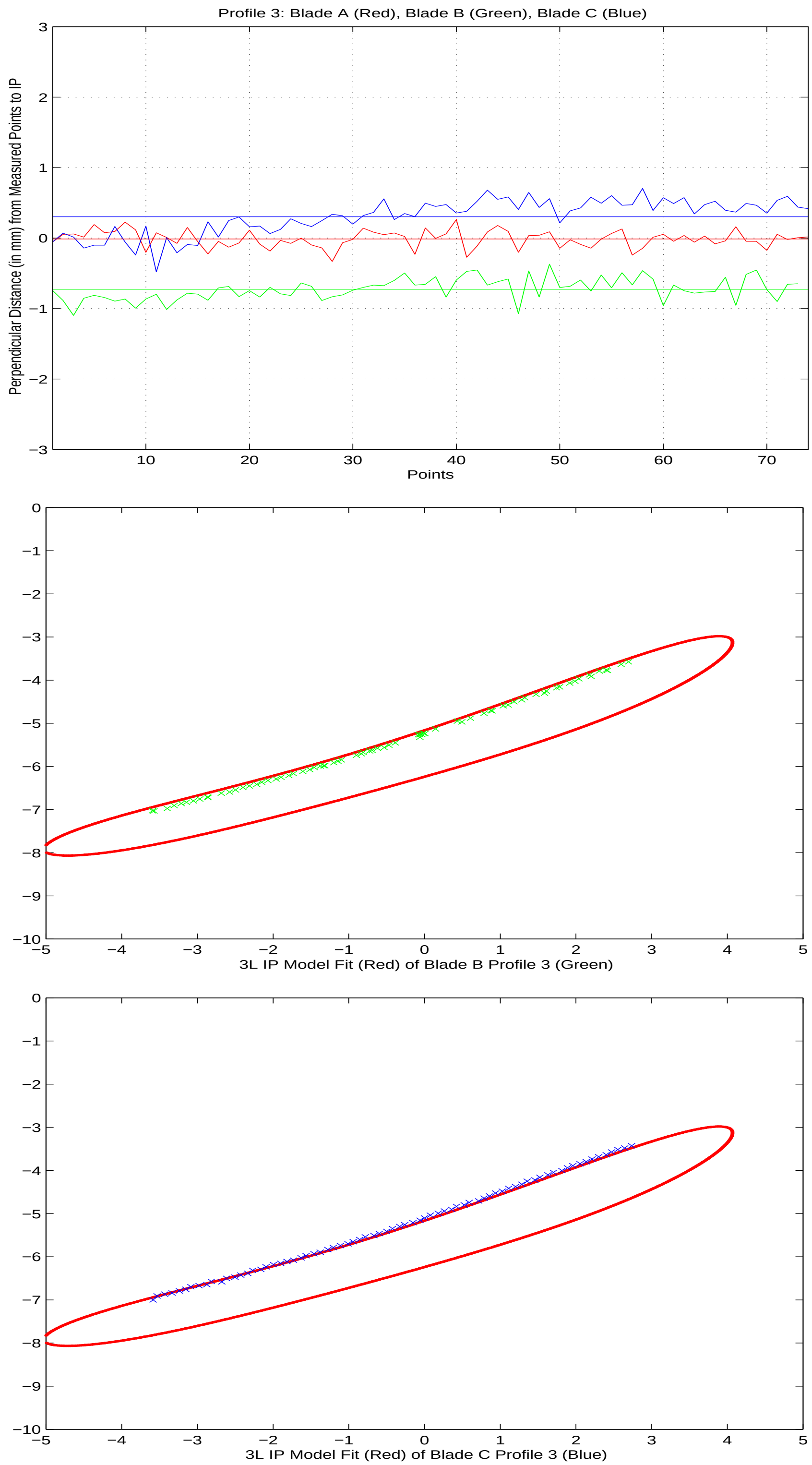

Figure 5: Profile 3 Perpendicular Distances

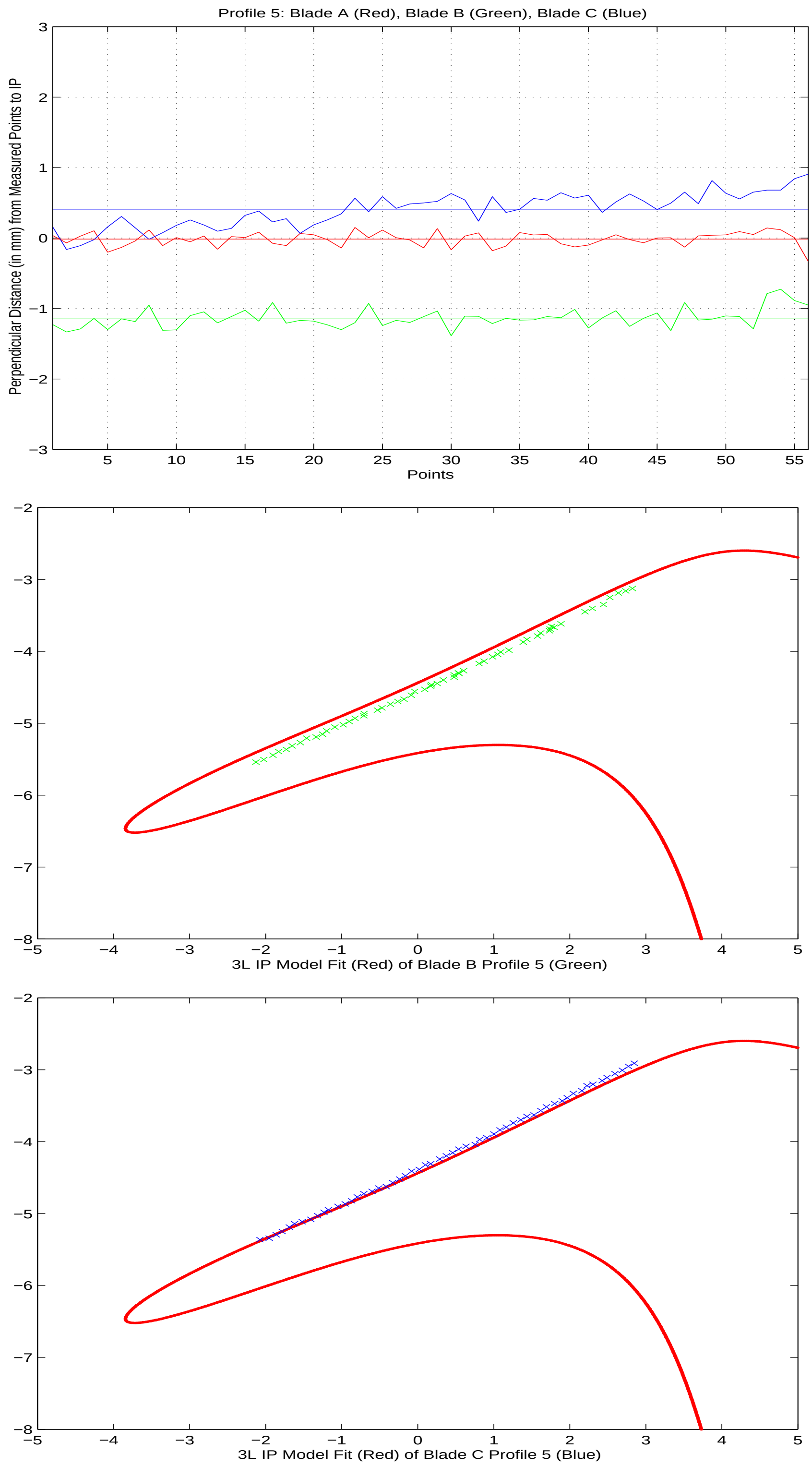

Figure 6: Profile 5 Perpendicular Distances

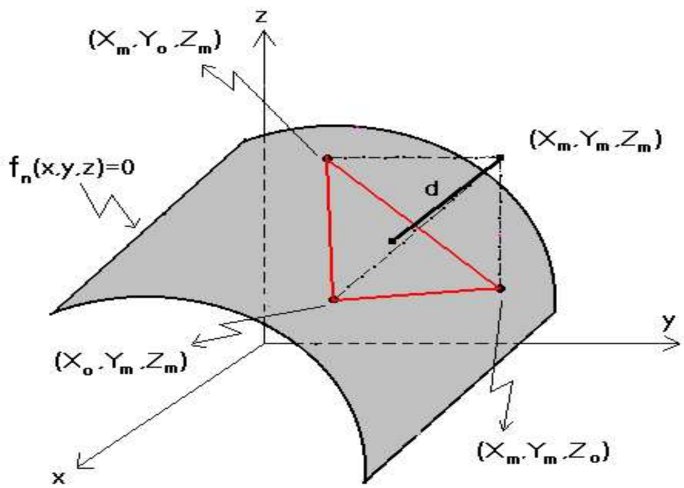

Figure 7: Determining ≈ 3-D ⊥ Distance Errors

$F_b(y, z)$. An entire 3-D model surface through several IP parallel profiles can be defined using such an interpolation strategy, which is particularly useful when the parallel profiles are relatively close to one another, as is the case here[3].

This interpolation procedure was employed to obtain a model 3-D IP surface between the five parallel profiles of blade A. Moreover, perpendicular measurement errors along arbitrary 3-D profiles then can be determined using such models and a 3-D "extension" of our 2-D measurement strategy, as depicted in Figure 7.

In particular, the equation of the plane through (x_0, y_m, z_m), (x_m, y_0, z_m) and (x_m, y_m, z_0) is defined by

$$det \begin{bmatrix} x - x_0 & y - y_m & z - z_m \\ x_m - x_0 & y_0 - y_m & 0 \\ x_m - x_0 & 0 & z_0 - z_m \end{bmatrix} = 0,$$

or

$$\underbrace{(y_m - y_0)(z_m - z_0)}_{a}(x - x_0) + \underbrace{(x_m - x_0)(z_m - z_0)}_{b}(y - y_m)$$

[3]In cases involving more complex shapes, quadratic, or higher order, interpolation procedures might be used to produce more representative surfaces between the defined profiles.

$$+ \underbrace{(x_m - x_0)(y_m - y_0)}_{c}(x_m - x_0) = 0,$$

where a, b and c define the normal direction to the plane[35]. The line through the measured point (x_m, y_m, z_m) perpendicular to this plane is then defined by

$$\frac{x - x_m}{a} = \frac{y - y_m}{b} = \frac{z - z_m}{c}$$

Substituting $(x - x_m)b/a + y_m$ for y and $(x - x_m)c/a + z_m$ for z into $f_n(x, y, z) = 0$ implies a polynomial equation in x alone which can readily be solved for x_f using Newton's root-finding procedure, as in the 2-D case. The corresponding y_f and z_f are subsequently given by $(x_f - x_m)b/a + y_m$ and $(x_f - x_m)c/a + z_m$, respectively, with the approximate distance between (x_m, y_m, z_m) and the IP surface given by

$$d = \sqrt{(x_m - x_f)^2 + (y_m - y_f)^2 + (z_m - z_f)^2}$$

This procedure was employed to determine the perpendicular distance errors from a 3-D interpolated IP model of blade A to analogous (x, y, z) trajectories along all 3 blades. These trajectories, which were chosen in a plane perpendicular to the (x, y)-plane and parallel to the z axis, are depicted in Figure 8 looking down the z axis. Although they appear as straight lines, because they lie in planes parallel to the z axis, they are curves.

The distance errors, which are plotted in Figure 9 using the IP surface equations obtained by interpolation at the beginning of this section, confirm our earlier 2-D profile observations. In particular, we again note that blade A has the smallest errors relative (of course) to its own model. Moreover the blade B errors are slightly (0 - 1.7 mm) below those of blade A, while the blade C errors are slightly (0 - 1.1 mm) above those of blade A.

5 Conclusions

We have now described the use of implicit polynomial models for modeling and measuring free-form curves and surfaces, primarily those characterized by repetitive shapes. Our result-s employed the 3L fitting algorithm in [25], which represents a fast and accurate fitting of

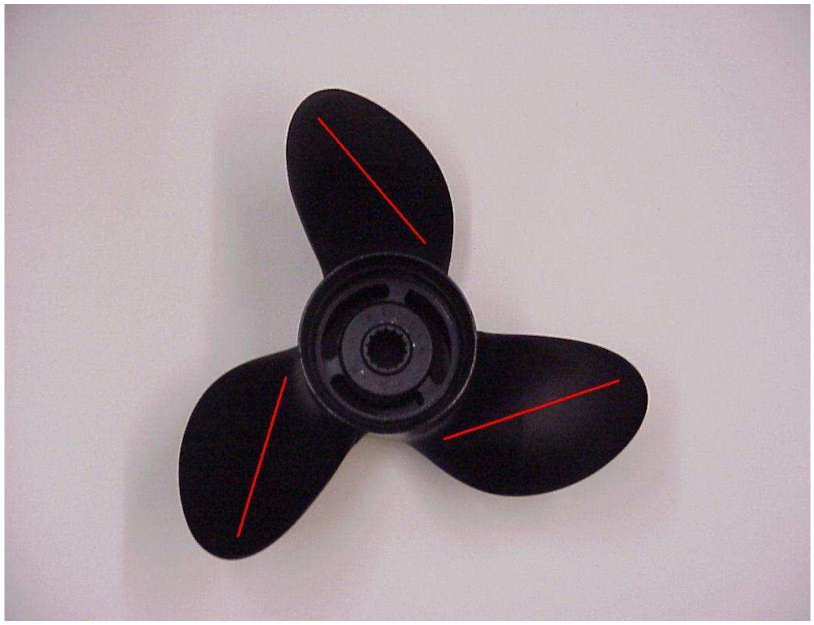

Figure 8: Analogous 3-D Trajectories

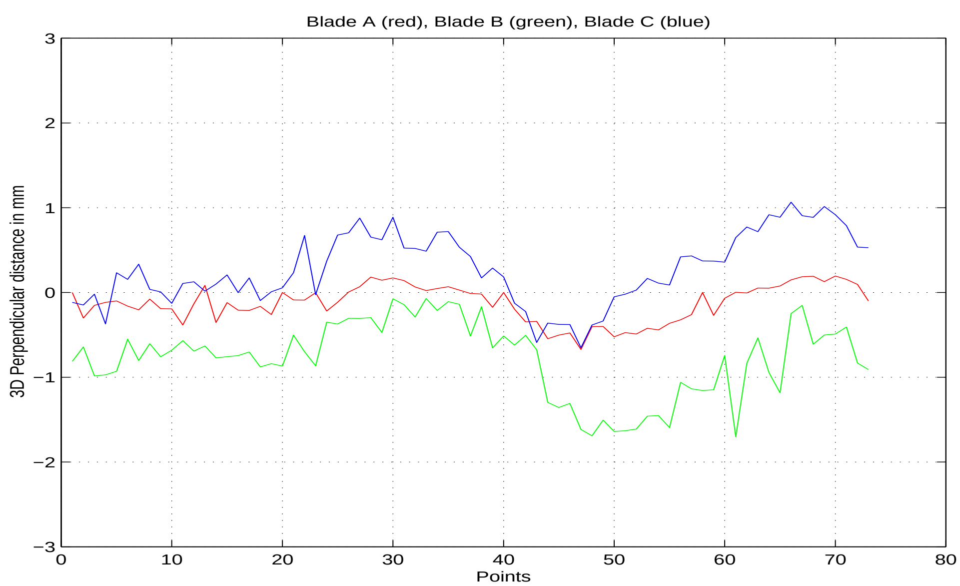

Figure 9: 3-D Distance Errors to Model Surface

measured 2-D points to corresponding implicit polynomial equations. Several parallel, two dimensional IP profiles were used to quantify the perpendicular distance errors between a model and measured propeller blades. The results were then extended to 3-D profiles using IP interpolation and a fast perpendicular surface error measurement algorithm. In summary, we illustrated how our new model-based measurement procedure can be used to quickly and accurately determine the distance errors between model shapes and "identical" manufactured shapes.

References

[1] Farin, Gerald, **Curves and Surfaces for CAGD: A Practical Guide** (Third Edition), Academic Press, 1993.

[2] Mortenson, Michael E., **Geometric Modeling** (Second Edition), Wiley Computer Publishing, 1997.

[3] Yamaguchi, Fujio, **Curves and Surfaces in Computer Aided Geometric Design**, Springer-Verlag, 1988.

[4] Patrikalakis, N. M., and Bardis, L., 1991, "Localization of Rational B-Spline Surfaces," Engineering with Computers, Vol. 7, pp. 237-252.

[5] S. T. Tuohy, T. Maekawa , G. Shen, N. M. Patrikalakis, "Approximation of measured data with interval B-splines," Computer-Aided Design, Vol. 29, No. 11, pp. 791-799, 1997.

[6] Wang, Y., "Minimum Zone Evaluation of Form Tolerances," Manufacturing Review, Vol. 5, No. 3, pp 213-220, 1992.

[7] Y. Wang, S. Gupta, F. Hulting, and P. Fussell, "Manufactured part modeling (MPM) for characterization of geometric variations of automotive spaceframe extrusions," Journal of Manufacturing Science and Engineering, ASME Trans., 120(3), 523-531, 1998.

[8] Choi, W., Kurfess, T. R., "Dimensional Measurement Data Analysis Part I, a Zone Fitting Algorithm," ASME Journal of Manufacturing Science and Engineering, Vol. 121, No. 2, pp. 238-245, May 1999.

[9] Choi, W., Kurfess, T. R., "Dimensional Measurement Data Analysis Part II, Minimum Zone Evaluation Design," ASME Journal of Manufacturing Science and Engineering, Vol. 121, No. 2, pp. 246-250, May 1999.

[10] Sahoo, K. C. and Menq, C. H., "Localization of 3-D objects having complex sculptured surfaces using tactile sensing and surface description," Journal of Engineering for Industry, 1991, 113, 85-92.

[11] Kurfess, T. and Banks, D., Statistical verification of conformance to geometric tolerance. Computer-Aided Design, 1995, 27(5), 353-361.

[12] Choi, W., Kurfess, T. R., "Uncertainty of Extreme Fit Evaluation for Three Dimensional Measurement Data Analysis," Computer-Aided Design, Vol. 30, No. 7, pp. 549-557, June 1998.

[13] Bispo, Edvaldo M. and Robert B. Fisher, "Free-Form Surface Matching for Surface Inspection," **The Mathematics of Surfaces VI**, Clarendon Press, 1996, pp. 119-136.

[14] Chazelle, Bernard, "Application Challenges to Computational Geometry," CG Impact Task Force Report, Department of Computer Science, Princeton University, Princeton, NJ, 1997.

[15] Hoffmann, Christoph M., **Geometric & Solid Modeling**, Morgan Kaufmann Publishers, Inc., 1989.

[16] Sederberg, T. W., D. C. Anderson and R. N. Goldman, "Implicit Representation of Parametric Curves and Surfaces," *Computer Vision, Graphics and Image Processing*, pp. 72-84, Academic Press, 1984.

[17] Bloomenthal, Jules, **Proceedings of Implict Surfaces '98**, *The Third International Workshop on Implicit Surfaces*, Seattle, Washington, June 15-16, 1998.

[18] Tarel, Jean-Phillipe, William A. Wolovich and David B. Cooper, "Covariant-Conics Decomposition of Quartics for 2D Object Recognition and Affine Alignment," Proceedings of the *1998 IEEE International Conference on Image Processing*, October 4-7, 1998, Chicago, Illinois.

[19] Unel, Mustafa and William A. Wolovich, "Complex Representations of Algebraic Curves," Proceedings of the *1998 IEEE International Conference on Image Processing*, October 4-7, 1998, Chicago, Illinois.

[20] Unel, Mustafa and William A. Wolovich, "Pose Estimation and Object Identification Using Complex Algebraic Representations," *Pattern Analysis and Applications*, (1998)1:178-188.

[21] Unel, Mustafa and William A. Wolovich, "Fitting Circle Polynomials to Planar Objects," Proceedings of the *First International Workshop on Computer Vision, Pattern Recognition and Image Processing*, October 23-28, 1998, Research Triangle Park, NC.

[22] Unel, Mustafa and William A. Wolovich, "Shape Control Using Primitive Decompositions," Proceeding of the *1999 International Conference on Shape Modeling and Applications*, March 1-4, 1999. Aizu-Wakamatsu, Japan.

[23] Wolovich, William A. and Mustafa Unel "The Determination of Implicit Polynomial Canonical Curves," *IEEE Transactions on Pattern Analysis and Machine Intelligence*, Vol. 20, No. 10, pp. 1080-1089, October 1998.

[24] Wolovich, William A. and Mustafa Unel, "Vision-Based System Identification and State Estimation," **The Confluence of Vision and Control**, Lecture Notes in Control and Information Systems 237, Springer 1998, pp. 171-182.

[25] Lei, Z., M. M. Blane, and D. B. Cooper, "The 3L Algorithm for Fitting Implicit Polynomial Curves and Surfaces to Data," *IEEE Transactions on Pattern Analysis and Machine Intelligence*, Vol. 22, No. 3, pp. 298-313, March 2000.

[26] Redding, R. J. and R. Whatmough, "Fitting Implicit Quartics For Use In Feature Extraction," Proceedings of the *International Conference on Image Processing*, Santa Barbara, CA. October, 1997.

[27] Tarel, Jean-Phillipe, Hakan Civi and David B. Cooper, "Pose Estimation of Free-Form 3D Objects without Point Matching using Algebraic Surface Models," Technical Report LEMS-167, September, 1997.

[28] Taubin, G., F. Cukierman, S. Sullivan, J. Ponce and D.J. Kriegman, "Parameterized Families of Polynomials for Bounded Algebraic Curve and Surface Fitting," *IEEE Transactions on Pattern Analysis and Machine Intelligence*, Vol. 16, No. 3, March, 1994.

[29] Bosch, John A., **Coordinate Measuring Machines and Systems**, Marcel Dekker, Inc., 1995.

[30] Taubin, Gabriel, "Estimation of Planar Curves, Surfaces, and Nonplanar Space Curves Defined by Implicit Equations with Applications to Edge and Range Image Segmentation," *IEEE Transactions on Pattern Analysis and Machine Intelligence*, Vol. 13, No. 11, pp. 1115-1137, November 1991.

[31] Boissonnat, J. D. "Shape Reconstruction from Planar Cross-Sections," *Computer Vision, Graphics and Image Processing,* 44 (1988). pp. 1-29.

[32] Castillo, Enrique and Andres Iglesias, "Some Characterizations of Families of Surfaces Using Functionsl Equations," *ACM Transactions on Graphics*, Vol. 16 (3), July, 1997, pp. 296-318.

[33] Muller, H. and A. Klingert, "Surface Interpolation from Cross Sections," **Focus on Scientific Visualization**, Springer-Verlag, 1993. pp. 130-189.

[34] Schumaker, Larry L., "Reconstructing 3D Objects from Cross-Sections," **Computation of Curves and Surfaces**, Kluwer Academic Publishers, 1990. pp. 275-309.

[35] CRC Standard Mathematical Tables and Formulae, 30th Edition, CRC Press, 1996, pp. 305.